Modulation-amplitude-locked laser diode interferometry for distance measurement

Takamasa Suzuki*, Tatsuo Iwana, and Osami Sasaki
Niigata University, Faculty of Engineering
8050 Ikarashi 2, Niigata City, 950-2181, Japan

ABSTRACT

This paper describes a range-finder that uses two feedback loops. Each feedback loop is respectively used to control the phase and the modulation-amplitude in a sinusoidal phase-modulating interference signal. It enables us to perform unambiguous measurement and real-time processing on the interference signal. Also external disturbance superimposed on the interference signal is eliminated by the feedback control. A distributed-Bragg-reflector laser diode that has wide range in wavelength-tuning allows us to improve the measurement accuracy.

Keywords: interferometry, distributed-Bragg-reflector laser diode, feedback control, sinusoidal phase modulation

1. INTRODUCTION

Ordinary interferometers cannot detect the distance that is larger than a half wavelength. Many kinds of approaches have been proposed to overcome this problem. Some of the most common approaches are multiple-wavelength interferometries that use two or more wavelengths. Generally, as two-wavelength interferometers use two separate laser sources[1, 2], it is difficult to align the optical axes, and setup is complicated. In such cases, wavelength tunability of a laser diode (LD) is very useful. That is, we can use different wavelengths with a single LD. For instance, quasi-two-wavelength interferometries (QTWIs) that use a single LD have been proposed and a step-profile measurement were demonstrated[3, 4]. In this measurement, we used "phase-locked" LD interferometry[5, 6]; a method capable of measuring surface profiles as well as distance, through feedback control. Although the optical setup in these devices is simple, measurement accuracy is restricted by the small wavelength-difference obtained. Moreover, the phase itself is sensitive to changes in optical path difference (OPD). It is difficult to conduct distance measurement with high resolution.

On the other hand, compared with the phase, the modulation-amplitude is less sensitive to changes in the OPD. Some approaches, for example double sinusoidal phase-modulating (DSPM) interferometers[7, 8], use this feature to the distance measurement. In these interferometers, two different sinusoidal signals are used to modulate the interference signal. The distance is measured from the modulation-amplitude in the sinusoidal phase-modulating (SPM) interference signal by use of frequency analysis. But it is difficult to implement the measurement in real-time because a lot of calculations are required in a computer.

In this paper, "modulation-amplitude-locked" laser diode interferometry, which uses a distributed-Bragg-reflector (DBR) LD is described. We control not only the phase but also the modulation-amplitude in the SPM interference signal by means of electronic circuit. Measurement ambiguity caused by phase-wrapping is thereby eliminated. Combined phase- and modulation-amplitude-locks allow us to stabilize the interference signal and achieve real-time signal processing. Moreover, measurement accuracy is improved, because the DBR LD's wavelength-tuning range is much wider than that of ordinary LDs[8, 9].

2. PRINCIPLE

2.1 FLOW OF SIGNAL PROCESSING

Experimental setup is shown in Fig. 1. We used a Fizeau interferometer, which consists of beam splitter BS2 as a

* Correspondence: E-mail: takamasa@eng.niigata-u.ac.jp; phone/fax: +81-25-262-7215;
Niigata University, 8050 Ikarashi 2, Niigata, 950-2181 JAPAN

Two- and Three-Dimensional Vision Systems for Inspection, Control, and Metrology, edited by Bruce G. Batchelor, Heinz Hügli, Proceedings of SPIE Vol. 5265 (SPIE, Bellingham, WA, 2004) · 0277-786X/04/$15 · doi: 10.1117/12.518640

reference and mirror M as an object, to demonstrate the distance measurements. Its initial OPD is 2L. The oscillator (OSC) serves the fundamental sinusoidal signal

$$I_b(t) = b\cos\omega_c t. \quad (1)$$

When the wavelength of the laser-source is modulated by

$$I_m(t) = a\cos\omega_c t, \quad (2)$$

the SPM interference signal

$$S(t) = S_{dc}+S_0\cos[z(t)\cos\omega_c t+\alpha(t)] \quad (3)$$

is generated[10], where $I_m(t)$ is the amplitude-controlled $I_b(t)$,

$$z(t) = 4\pi a\beta[L+d(t)]/\lambda_0^2 \quad (4)$$

is the modulation-amplitude, and

$$\alpha(t) = 4\pi d(t)/\lambda_0 \quad (5)$$

is the phase that depends on both OPD and wavelength. S_{dc}, S_0, β, $d(t)$, and λ_0 represent background intensity, amplitude of the interference signal, modulation efficiency, temporal displacement of the object, and the central wavelength, respectively.

We first eliminate dc component or the background intensity S_{dc} from S(t) by using a high-pass filter (HPF). Generally the second term in Eq. (3), however, contains not only ac component but also dc one. We control the phase $\alpha(t)$ so as to convert the second term to pure ac component. When the phase $\alpha(t)$ is controlled to $-\pi/2$ by the control current $I_c(t)$, Eq. (3) is expressed by

$$S_1(t) = S_{dc}+S_0\sin[z(t)\cos\omega_c t]. \quad (6)$$

Then we can easily derive the second term from Eq. (6) by using a HPF as follows:

$$S_2(t) = S_0\sin[z(t)\cos\omega_c t]. \quad (7)$$

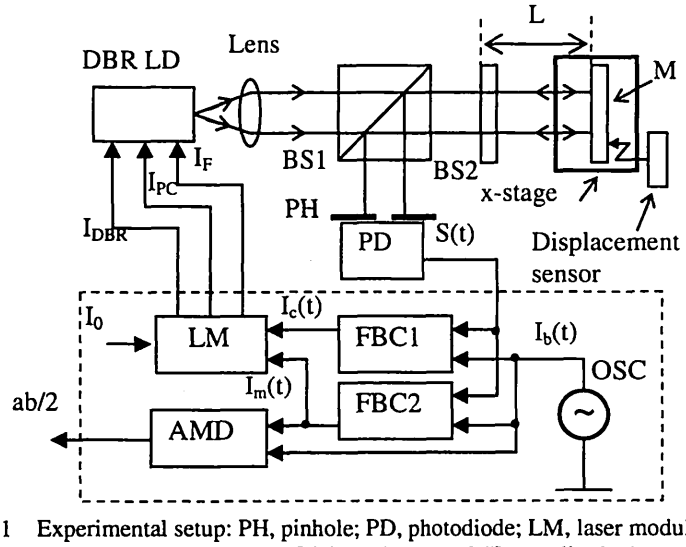

Fig. 1 Experimental setup: PH, pinhole; PD, photodiode; LM, laser modulator; FBC, feedback controller; OSC, oscillator; AMD, amplitude detector.

Next, if the modulation-amplitude z(t) in signal $S_2(t)$ is controlled to π, we have

$$S_3(t) = S_0 \sin[\pi \cos \omega_c t]. \quad (8)$$

From Eq. (4), distance is given by

$$[L+d(t)] = \lambda_0^2/4a\beta \quad (9)$$

under the condition represented by Eq. (8).

Thus, the amplitude 'a' is given by the product

$$I_b(t) \times I_m(t) = ab/2 + (ab/2)\cos[2\omega_c t]. \quad (10)$$

If the first term ab/2 is extracted by means of a low-pass filter (LPF), we can easily detect the amplitude 'a' because b/2 is constant. This processing is implemented in the amplitude detector AMD, which is illustrated in Fig. 2.

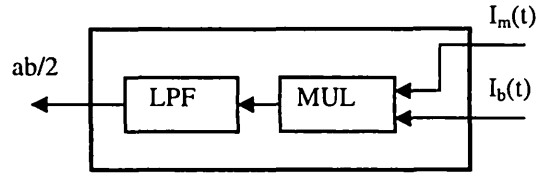

Fig. 2 Block diagram of the AMD: MUL, multiplier; LPF, low-pass filter.

2.2 PHASE-LOCK AND MODULATION-AMPLITUDE-LOCK

Both phase-lock and modulation-amplitude-lock are implemented by the respective feedback controls. Although process of the phase-lock has already been explained in other references[4-6], we briefly explain it.

Block diagram of feedback controller FBC1 is shown in Fig. 3. It consists of an frequency doubler (FRD), a multiplier, an LPF, and a proportional-integral (PI) controller (PI1). The FRD doubles the frequency of $I_b(t)$. The output of the FRD is given by $I_{b2}(t)$. Multiplying S(t) and $I_{b2}(t)$ and passing the product through the LPF, as shown in Fig. 3, we have feedback signal

$$F_1(t) = K\cos\alpha(t), \quad (11)$$

where $K = -S_0 b^2 J_2(z)/2$ and $J_2(z)$ is the second order Bessel function. PI1 generates control current $I_c(t)$ so as to realize the condition of $F_1(t) = 0$. When the control current $I_c(t)$ is injected into the LD, phase $\alpha(t)$ is automatically adjusted to $-\pi/2$. Thus S(t) is converted to $S_1(t)$.

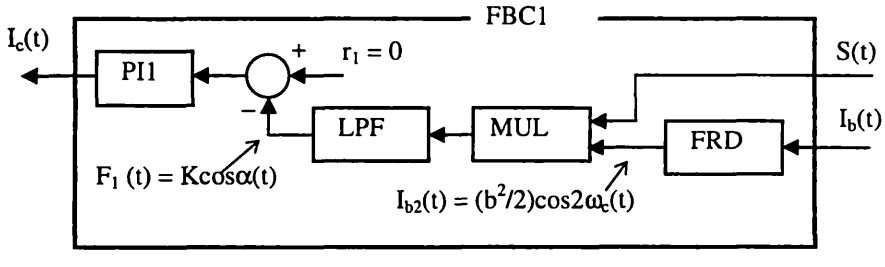

Fig. 3 Block diagram of the FBC1: FRD, frequency doubler; PI1, proportional-integral controller.

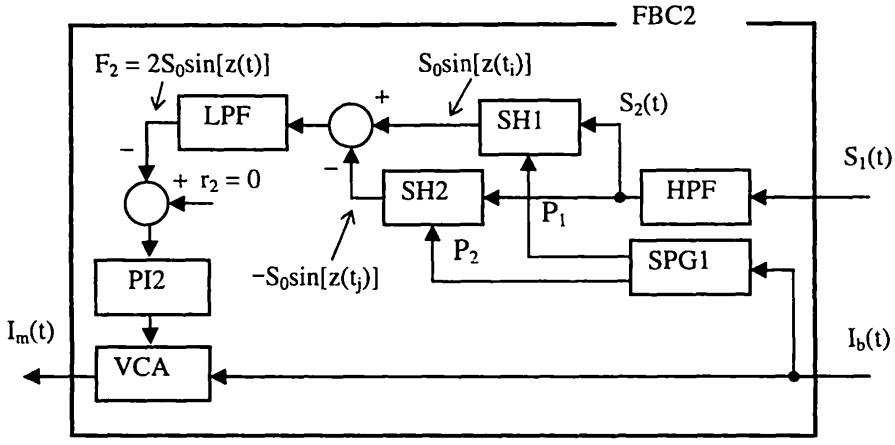

Fig. 4 Block diagram of the FBC2: HPF, high-pass filter; SH, sample-and-hold circuit; SPG, sampling pulse generator; VCA, voltage controlled amplifier; PI2, proportional-integral controller.

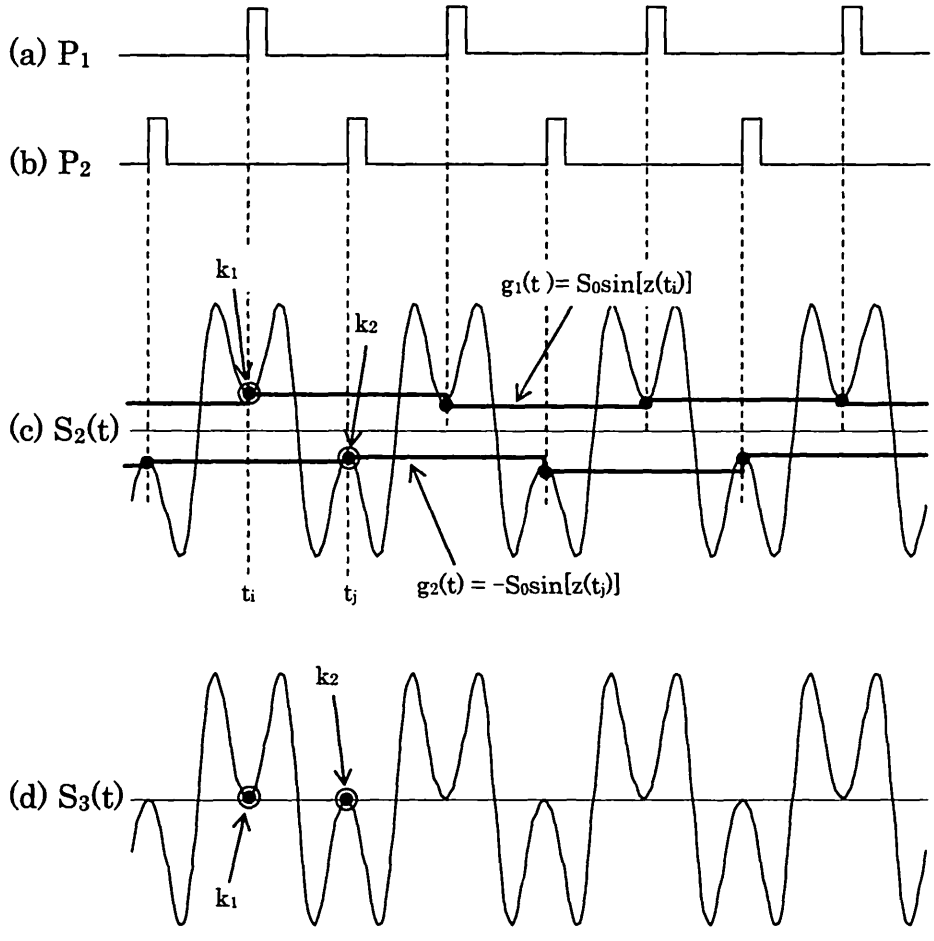

Fig. 5 Schematic of the feedback control. By use of sampling pulses (a) P_1 and (b) P_2, sample-and-hold circuits sample (c) $S_2(t)$. Phase change from k_1 to k_2 on S(t) becomes π and (d) $S_3(t)$ is obtained.

Figure 4 indicates the block diagram of feedback controller FBC2 that controls the modulation-amplitude. The HPF extracts $S_2(t)$ from $S_1(t)$. Sampling pulse generator SPG serves the pulse trains P_1 and P_2 at $t_i = 2i\pi/\omega_c$ and $(2j+1)\pi/\omega_c$, respectively, as shown in Figs. 5(a) and 5(b), where i and j are whole numbers. If $S_2(t)$ is alternately sampled and held at the time t_i and t_j by using sample-and-hold circuits SH1 and SH2, we obtain two separate signals $g_1(t) = S_0\sin[z(t_i)]$ and $g_2(t) = -S_0\sin[z(t_j)]$ as shown in Fig. 5(c), because $\cos\omega_c t$ becomes ± 1 at t_i and t_j. Subtracting the latter from the former and passing it through a LPF, we obtain feedback signal

$$F_2(t) = 2S_0\sin[z(t)]. \qquad (12)$$

We control $F_2(t)$ to be zero by use of PI controller PI2. In this time amplitude of $I_b(t)$ is properly adjusted with a voltage-controlled amplifier (VCA) and modulating current $I_m(t)$ locks the modulation-amplitude z(t) to π. That is, the levels of $g_1(t)$ and $g_2(t)$ coincide with each other. Then the phase change from k_1 to k_2 on S(t) becomes π as shown in Fig. 5(d).

3. EXPERIMENT

In this experiment, we used the DBR LD (YOKOGAWA YL85XTW) whose operating wavelength and maximum output power are ~853 nm and 5 mW, respectively. This device possesses three electrodes that inject forward current I_F, phase tuning current I_{PC}, and reflection-tuning current I_{DBR}. Bias current I_0 and two control currents $I_c(t)$ and $I_m(t)$ are injected into the DBR LD through the LD modulator LM as shown in Fig. 1. The optical power mainly depends on I_F. Wavelength varies widely according to I_{DBR} without mode-hopping when the ratio between I_{PC} and I_{DBR} is maintained at 1:1.4-1.5. The wavelength variation on I_{PC} is traced in Fig. 6. The inclination shows that the modulation efficiency β is estimated to be 1.90×10^{-2} nm/mA. The range of wavelength change is ~2 nm. In the dynamic usage, however, the efficiency β drops because it depends on modulating frequency[8]. When we modulated the DBR LD with an 18 kHz sinusoidal signal in the experiment, it became 6.55×10^{-3} nm/mA.

We first checked waveforms in the series of signal processing as shown in Fig. 7. The interference signal S(t) contains dc component in both background signal and temporally changing signal as shown in Fig. 7(a) when no feedback controls are implemented. Also external disturbance is superimposed on S(t). When the phase-lock control is applied on S(t), the waveform becomes symmetric as shown in Fig. 7(b). We can find that the dc component in the temporally changing signal and the disturbance are eliminated. Passing $S_1(t)$ through the HPF as shown in Fig. 4, we have $S_2(t)$, in which all dc component are removed (Fig. 7(c)). Moreover, as shown in Fig. 7(d), z(t) becomes π, when the modulation-amplitude-lock control is implemented. Amplitude-controlled modulating signal $I_m(t)$ that realizes modulation-amplitude-lock in Fig. 7(d) is traced in Fig. 7(e). The distance was calculated by use of Eq. (9) after detecting the amplitude of $I_m(t)$.

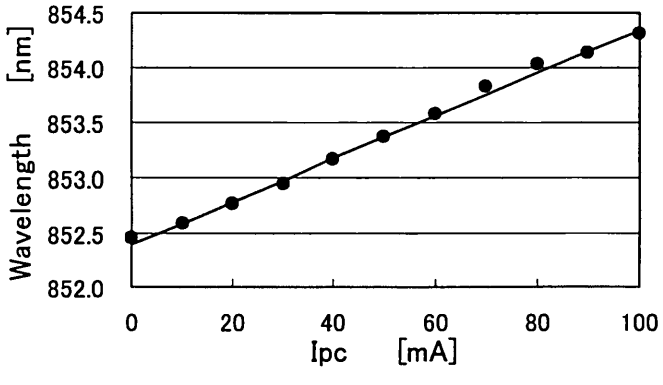

Fig. 6 DBR LD wavelength change according to I_{PC}. The ratio between I_{PC} and I_{DBR} is 1:1.4.

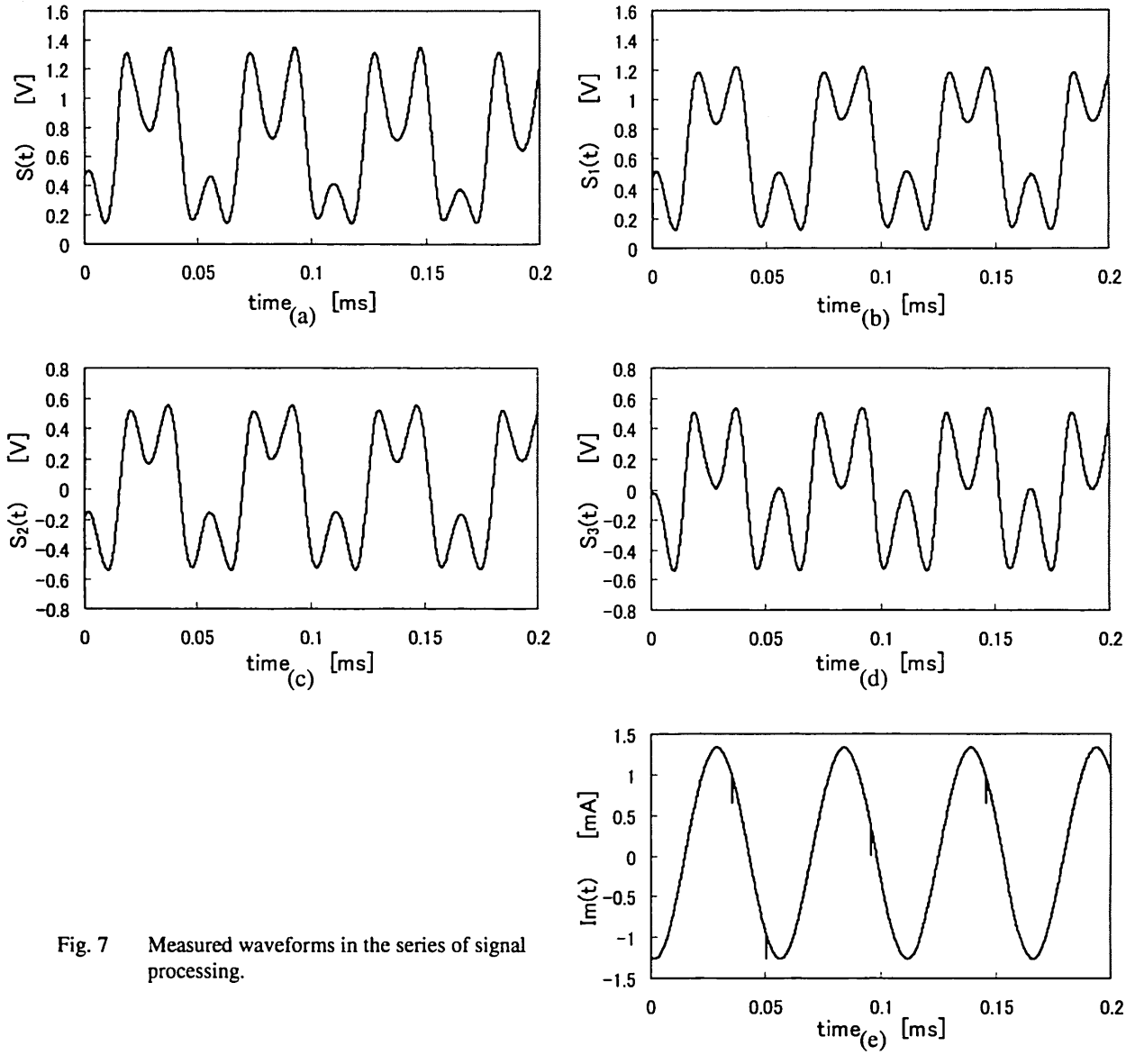

Fig. 7 Measured waveforms in the series of signal processing.

Next, we measured the position of the mirror. This mirror was mounted on the x-axis stage in such a way that allowed it to move along the optical axis. At the same time, displacements were monitored by a dedicated sensor whose resolution was 0.1 μm. We moved the mirror from L to L+0.8 mm, in discrete 0.1 mm increments, where L was set to 7.145 mm. Results are shown in Fig. 8. The deviation in these measurements was estimated to be 14.3 μm in this prototype. This error will be decreased if the control parameters are suitably tuned and improve the accuracy for the modulation-amplitude detection.

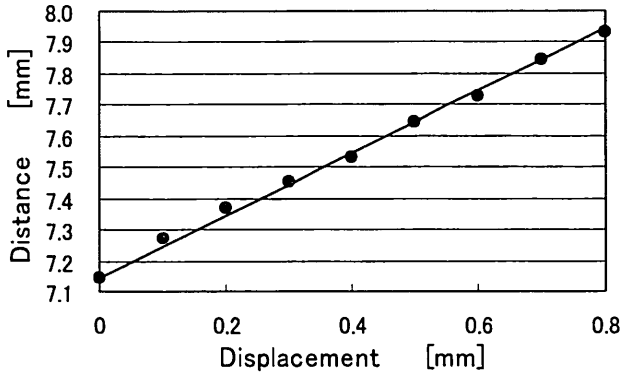

Fig. 8 Distance measured at intervals of 0.1 mm.

4. CONCLUSIONS

A simple range finder that uses a distributed-Bragg-reflector LD is proposed and demonstrated. Both phase-lock and modulation-amplitude-lock controls enable us to convert waveform of the interference signal to the desired ones. It results in real-time distance measurement. Our preliminary experiments indicate a measurement error of 14.3 μm in rms.

REFERENCES

1. Y.-Y. Cheng, and J. C. Wyant, "Two-wavelength phase shifting interferometry," *Appl. Opt.* **23**, 4539-4543 (1984).
2. A. J. den Boef, "Two-wavelength scanning spot interferometer using single-frequency diode lasers," *Appl. Opt.* **27**, 306-311 (1988).
3. C. C. Williams and H. K. Wickramasinghe, "Optical ranging by wavelength multiplexed interferometry," *J. Appl. Phys.* **60**, 1900-1903 (1986).
4. T. Suzuki, T. Muto, O. Sasaki, and T. Maruyama, "Wavelength-multiplexed phase-locked laser diode interferometer using a phase-shifting technique," *Appl. Opt.* **36**, 6196-6201 (1997).
5. T. Suzuki, O. Sasaki, and T. Maruyama, "Phase-locked laser diode interferometry for surface profile measurement," *Appl. Opt.* **28**, 4407-4410 (1989).
6. T. Suzuki, O. Sasaki, and T. Maruyama, "Absolute distance measurement using wavelength-multiplexed phase-locked laser diode interferometry," *Opt. Eng.* **35**, 492-497 (1996).
7. O. Sasaki, T. Yoshida, and T. Suzuki, "Double sinusoidal phase-modulating laser diode interferometer for distance measurement," *Appl. Opt.* **30**, 3617-3621 (1991).
8. T. Suzuki, H. Suda, and O. Sasaki, "Double sinusoidal phase-modulating distributed- Bragg-reflector laser-diode interferometer for distance measurement," *Appl. Opt.* **42**, 60-66 (2003).
9. G. Mourat, N. Servagent, and T. Bosch, "Distance measurement using the self-mixing effect in a three electrode distributed Bragg reflector laser diode," *Opt. Eng.* **39**, 738-743 (2000).
10. O. Sasaki, K. Takahashi, and T. Suzuki, "Sinusoidal phase modulating laser diode interferometer with a feedback control system to eliminate external disturbance," *Opt. Eng.* **29**, 1511-1515 (1990).